

### III. RESULTS AND CONCLUSIONS

A mathematical model of the steady-state behavior of the ALE has been presented that includes the effects of stationary time-varying random fluctuations in the ALE weights. This model of the ALE displays spectral broadening of input line components, as one would expect. The model is useful for predicting line spreading when the coherence time of ALE input is much longer than the length of the filter, as can occur if the ALE acts as a prefilter to a spectrum analyzer.

#### REFERENCES

- [1] J. T. Rickard and J. R. Zeidler, "Second-order output statistics of the adaptive line enhancer," *IEEE Trans. Acoust., Speech, Signal Processing*, vol. ASSP-27, pp. 31-39, Feb. 1979.
- [2] L. L. Horowitz and K. D. Senne, "Performance advantage of complex LMS for controlling narrowband adaptive arrays," *IEEE Trans. Circuits Syst.*, vol. CAS-28, June 1981.
- [3] N. J. Bershad, "On the real and complex LMS adaptive filter algorithms," *Proc. IEEE*, vol. 69, pp. 469-470, Apr. 1981.
- [4] B. Widrow, J. McCool, and M. Ball, "The complex LMS algorithm," *Proc. IEEE*, vol. 63, pp. 719-720, Apr. 1975.
- [5] B. Fisher and N. J. Bershad, "The complex LMS adaptive algorithm—Transient weight mean and covariance with applications to the ALE," *IEEE Trans. Acoust., Speech, Signal Processing*, vol. ASSP-31, pp. 34-44, Feb. 1983.
- [6] B. Fisher, "Transient statistical behavior of the LMS adaptive predictor with applications to sinusoidal inputs," Ph.D. dissertation, Univ. California, Irvine, June 1980.
- [7] B. Fisher and N. J. Bershad, "ALE behavior for two sinusoidal signal models," *IEEE Trans. Acoust., Speech, Signal Processing*, to be published.
- [8] N. J. Bershad and Y. H. Chang, "Time correlation statistics of the LMS adaptive algorithm weights," *IEEE Trans. Acoust., Speech, Signal Processing*, to be published.
- [9] Y. H. Chang, "Time correlation statistics of the LMS adaptive algorithm weights and applications," Ph.D. dissertation, Univ. California, Irvine, June 1983.

### Generalization of the Window Method for FIR Digital Filter Design

A. DEMBO AND D. MALAH

**Abstract**—A generalization of the conventional window method for the design of finite impulse response (FIR) digital filters is presented by including nonequal passband and stopband ripple specifications in the design process. Typically, this results in a savings of up to 30 percent in filter length in comparison to the conventional approach.

#### I. INTRODUCTION

The window method for designing finite impulse response (FIR) digital filters is well known and widely used [1 pp. 88-104]. Its main advantage is its simplicity since it is an analytical technique. The disadvantages of the technique are that the design is not optimal in the min-max sense, and that there is no independent control on the design parameters. This usually results in the need for several design iterations with different window lengths and shapes until the design specifications are met.

Manuscript received August 28, 1983; revised April 18, 1984.

The authors are with the Department of Electrical Engineering, Technion—Israel Institute of Technology, Haifa 32000, Israel.

The approach presented in this work provides better control on the design parameters for the important class of multi-band bandpass/bandstop linear phase FIR digital filters. It typically results in savings of up to 30 percent (theoretically 50 percent) in filter length, and provides a better understanding of the relationship between the features of the window function and the designed filter. The new approach still preserves the simplicity of the original window method.

#### II. THE NEW DESIGN APPROACH

Consider the design of a low-pass (LP) filter. The ideal LP filter specifications are given by

$$H_d(f) = \begin{cases} 1 & |f| \leq F_c \\ 0 & F_c < |f| \leq 0.5 \end{cases} \quad (1)$$

where  $f$  is a normalized frequency variable (0.5 corresponds to half the sampling frequency).

The practical LP filter is specified in terms of the passband and stopband frequencies  $F_p$  and  $F_s$ , respectively, the peak passband ripple  $\delta_p$ , and the peak stopband ripple  $\delta_s$ , as follows:

$$\begin{aligned} 1 - \delta_p &\leq |H(f)| \leq 1 + \delta_p & |f| \leq F_p \\ 0 &\leq |H(f)| \leq \delta_s & F_s \leq |f| \leq 0.5 \end{aligned} \quad (2)$$

where  $F_s > F_p$  and  $[F_p, F_s]$  is the transition band. The width of the transition band is defined as

$$\Delta F = F_s - F_p. \quad (3)$$

In the conventional window method [1], [2],  $F_c$  is chosen to be at the center of the transition band. This results in equal deviations in the passband and stopband ( $\delta_p = \delta_s$ ). Since usually the specification is for  $\delta_p \neq \delta_s$ , the design by the conventional method is based on  $\delta_{\text{crit}} = \min(\delta_p, \delta_s)$ .

The basic idea of the new approach is to properly set  $F_c$  (not necessarily at the center of the transition band) so that the given deviation specifications can be satisfied (i.e.,  $\delta_p \neq \delta_s$ ) with a shorter filter length than needed with the conventional window method. This is the basic difference between the new approach and the conventional method. Once  $F_c$  is set to its optimal value, the remaining design procedure is exactly the same for both methods.

The basic idea is illustrated in Fig. 1. The dashed line shows the response of a filter designed using the conventional window method.  $F_c$  is at the center of the transition band  $[F_p, F_s]$  (denoted by  $\hat{F}_c$ ) and the filter is characterized by equal deviations in the passband and stopband ( $\delta_{\text{crit}} = \delta_s$ ). The solid line shows the filter response designed according to the proposed technique, i.e., using the optimal value of  $F_c$ , denoted by  $F_{c_{\text{opt}}}$ . Since  $F_{c_{\text{opt}}}$  is closer to  $F_p$  than to  $F_s$ , the frequency  $\tilde{F}_p$  at which  $|H(f)| = 1 - \delta_{\text{crit}}$  is less than  $F_p$ . Thus, effectively, the transition band is increased by  $\Delta F' = F_p - \tilde{F}_p$ .

It is well known [1] that an estimate for the needed filter length is given by  $\hat{M} \cong (\hat{D}/\Delta F) + 1$  where  $\hat{D}$  is the normalized window width (transition-band width times the window span [2]) and is a parameter which depends only on the deviation  $\delta_{\text{crit}}$  and the window type. Therefore, with the new design,  $M \cong \hat{D}/(\Delta F + \Delta F') + 1$ . If we now define  $D' \triangleq (M - 1)\Delta F'$ , we find

$$M \cong (\hat{D} - D')/\Delta F + 1. \quad (4)$$

To derive the optimal value of  $F_c$ , we first define the following variables:

$$\Delta F_p \triangleq F_c - F_p; \quad \Delta F_s \triangleq F_s - F_c \quad (5)$$

$$D_p \triangleq (M - 1)\Delta F_p; \quad D_s \triangleq (M - 1)\Delta F_s. \quad (6)$$

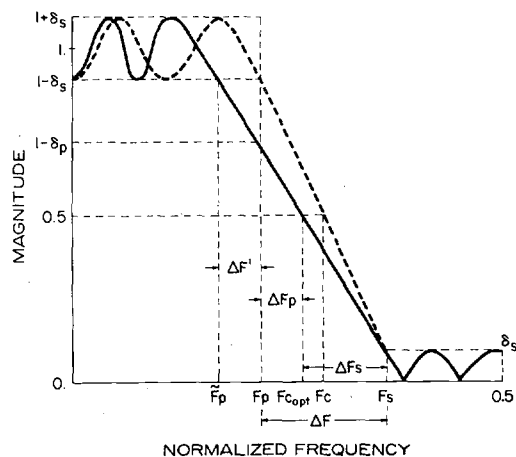


Fig. 1. Frequency response of typical filters designed by the conventional (dashed line) and new (solid line) window techniques.

Fig. 1 also illustrates the important fact that the optimal value of  $F_{c_{opt}}$  is exactly at the center of the extended transition band  $[F_p, F_s]$  (since  $|H(\tilde{F}_p)| = 1 - \delta_{crit}$ ), and therefore,  $\Delta F' = \Delta F_s - \Delta F_p$ .

It follows that

$$D_s = \hat{D}/2; \quad D_p = \hat{D}/2 - D', \quad (7)$$

and hence (4) can be rewritten as

$$M \cong (D_s + D_p) \Delta F + 1. \quad (8)$$

Finally, from (5) and (6), we can calculate the optimal value of  $F_c$  in terms of  $F_p, F_s, D_p, D_s$  by

$$F_{c_{opt}} = (D_s F_p + D_p F_s) / (D_p + D_s). \quad (9)$$

Note that if  $D_p = D_s$  (i.e.,  $\delta_p = \delta_s$ ), the result is  $F_{c_{opt}} = \hat{F}_c = (F_p + F_s)/2$ , as expected.

The above analysis was based on a filter for which  $\delta_p > \delta_s$  (which is the more common situation). However, (8) and (9) are general and hold also for  $\delta_s > \delta_p$ . Thus, there is no restriction on using the new design method with any specification of  $\delta_p$  and  $\delta_s$  for which  $\delta_p \neq \delta_s$ .

Since  $\hat{D} = 2 \max(D_s, D_p)$ , we find that

$$\frac{M}{\hat{M}} = \frac{1}{2} \left[ 1 + \frac{\min(D_s, D_p)}{\max(D_s, D_p)} \right], \quad (10)$$

and hence, in the limit, a savings of up to 50 percent in filter length can be obtained by the new method in comparison to the conventional window method.

The reason for expressing  $F_c$  in terms of  $D_s$  and  $D_p$  is that, as shown in the sequel,  $D_p$  and  $D_s$  can be easily found. Since  $H(f)$  is symmetric about  $F_c$ , it was found that  $D_p$  is related only to  $\delta_p$ , and  $D_s$  is related only to  $\delta_s$ . Furthermore, both  $D_p$  and  $D_s$  are related to  $\delta_p$  and  $\delta_s$ , respectively, by the same function [5], [6]. We found that it is more convenient to calculate the deviation  $\delta$  as function of the related normalized (and scaled by 1/2) window-width variable  $D$  rather than the other way around. This function, which we denote by  $\delta = I(D)$ , is independent of the filter length  $M$  for most practical values of  $M$  (e.g.,  $M \geq 21$ ) if the window sequence  $w(n)$ , for different values of  $M$ , is a sampled version of the same continuous-time function  $w_\alpha(t)$ . That is,  $w(n)$  is obtained from  $w_\alpha(t)$  by uniformly sampling the interval  $t \in [-1, 1]$  at a sampling interval of  $2/(M-1)$ . The shape of  $w_\alpha(t)$  defines the window type. Indeed, most popular windows can be considered as a sampled version of a continuous-time function so that the function  $I(D)$  is obtained by uniformly sampling the integrand

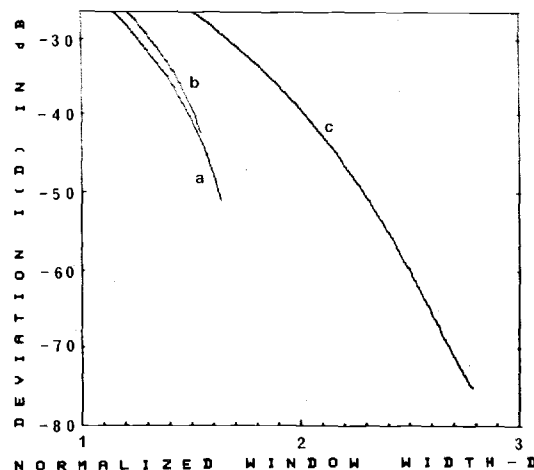


Fig. 2. The function  $\delta = I(D)$  for (a) Hamming, (b) Hann, and (c) Blackman windows.

of the integral in the definition of the function  $I_\alpha(D)$  below:

$$I_\alpha(D) = 0.5 \left\{ w_\alpha(0) - \int_{-1}^1 w_\alpha(t) \frac{\sin(\pi Dt)}{\pi t} dt \right\} \quad (11)$$

using a sampling interval of  $2/(M-1)$ .

In the derivation of (11), it is assumed that the passband and stopband are wide enough (in comparison to the transition band). If one of these bands is narrow, its width affects the value of  $D$  related to this band, and using the function  $I(D)$  derived from (11), which is independent of the filter frequency response, it yields a filter which does not satisfy the given specifications for  $(\delta_p, \delta_s)$ . A method for checking if the bands are wide enough and for modifying the specifications if the bands are not sufficiently wide is given in [6]. This modification allows using  $I(D)$  for the design of narrow-band filters as well. From this point on, we assume that the filter has sufficiently wide bands. Fig. 2 shows the function  $I(D)$  for the Hann, Hamming, and Blackman windows.

For the widely used Kaiser window family, an associated family of design curves is needed, i.e., a curve for each value of the window parameter  $\alpha$ . In [2, eq. (7)], an empirical relation is given for computing the optimal value of the window parameter for a given value of the critical deviation  $\alpha(\delta_{crit})$ . A second empirical relation [2, eq. (8)] evaluates the normalized transition-band width for a given value of the critical deviation  $\hat{D}(\delta_{crit})$ . Extensions of these two relations to estimate  $D_p$  and  $D_s$  for  $\delta_p \neq \delta_s$  are as follows [5], [6] (for  $\delta_p > \delta_s$ ):

$$D_s \cong \hat{D}(\delta_{crit} = \delta_s) / 2 \quad (12)$$

$$D_p \cong \hat{D}(\delta_{crit} = \delta_p) / 2 + [\alpha(\delta_{crit} = \delta_s) - \alpha(\delta_{crit} = \delta_p)] \cdot S(\delta_p) \quad (13)$$

where

$$S(\delta_p) = 0.105 - 0.00275(20 \log_{10} \delta_p + 21). \quad (14)$$

For  $\delta_s > \delta_p$ , the  $p$  and  $s$  subscripts in (12)–(14) are simply exchanged. The optimal window parameter  $\alpha$  is selected according to [2, eq. (7)]. The design is continued by using (8) and (9) to find the filter length  $M$  and to set  $F_{c_{opt}}$ .

From Fig. 1 it is seen that the response at the edge of the passband drops, as desired, to  $(1 - \delta_p)$ , but the maximum value of the response is less than the allowed value of  $(1 + \delta_p)$ . This asymmetry in the deviation about the value of 1 can be utilized to further reduce the filter length by properly modifying  $H_d(f)$ . Details of the design process which takes into

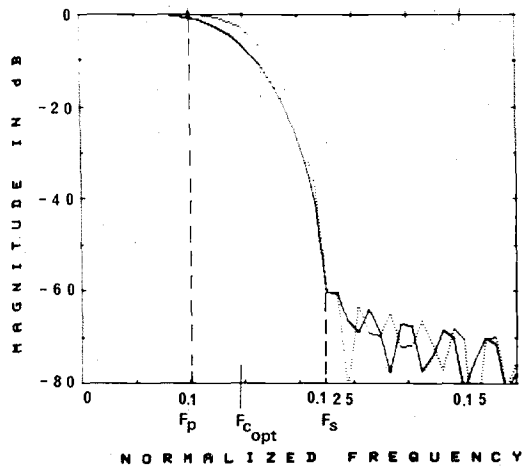


Fig. 3. Frequency response of filters designed by the conventional (dashed line,  $M=146$ ) and the new (solid line  $M=116$ ) window techniques for the same specifications ( $\delta_p = 0.057$  and  $\delta_s = 0.001$ ).

account this asymmetry are given in [6]. Typically, an additional 5–10 percent reduction in filter length is obtained.

To illustrate the new design approach, consider the design of a low-pass filter with the following specifications:  $F_p = 0.1$ ,  $F_s = 0.125$ ,  $\delta_p = 0.057$  (1 dB passband relative ripple),  $\delta_s = 0.001$  (60 dB stopband attenuation). An optimal equiripple filter design [3], [4] results in a filter length of 85. Using the conventional window design method ( $F_c = 0.1125$ ) with a Kaiser window ( $\alpha = 0.5653$ ) results in a filter length of  $M = 146$ . For the same specifications and the same Kaiser window, the new design approach results in a filter length of  $M = 116$ . The frequency response of the last two filters are compared in Fig. 3. It is of interest to note that if the asymmetry in deviation about 1 (at the passband) is utilized [6], the filter length is further reduced to 112.

## V. CONCLUSIONS

A generalization of the conventional window method was presented for the design of FIR digital filters with nonequal passband and stopband ripple specifications. The reduction in filter length depends on the mismatch between the passband and stopband specification, and can result, in the limit, in a savings of up to 50 percent, although practical specifications typically result in savings of 20–30 percent. The proposed technique preserves the simplicity of the conventional window method, and was shown to have a simple extension to multiband filter design, provided the bands are sufficiently separated. Known empirical design relations for the Kaiser window family [2] were extended to include the new approach, avoiding the need for an iterative design. The extension of the proposed generalization to the design of multiband bandpass/bandstop filters and the application of the new approach to the design of filter banks is given in [6]. Its application to the design of differentiators and Hilbert transform filters is in progress.

## REFERENCES

- [1] L. R. Rabiner and B. Gold, *Theory and Application of Digital Signal Processing*. Englewood Cliffs, NJ: Prentice-Hall, 1975.
- [2] J. F. Kaiser, "Nonrecursive digital filter design using the  $J_0$  - sinh window function," in *Proc. 1974 IEEE Int. Symp. Circuit Theory*, pp. 20–23.
- [3] O. Herrmann, L. R. Rabiner, and D.S.K. Chan, "Practical design rules for optimum finite impulse response lowpass digital filters," *Bell Syst. Tech. J.*, vol. 52, pp. 769–799, July–Aug. 1973.

- [4] J. H. McClellan, T. W. Parks, and L. R. Rabiner, "A computer program for designing optimum FIR linear phase digital filters," *IEEE Trans. Audio Electroacoust.*, vol. AU-21, pp. 506–526, Dec. 1973.
- [5] A. Dembo and D. Malah, "Generalization of the window method for FIR digital filter design," *IEEE 13th Conv. Elec. Electron. Eng. in Israel*, Tel-Aviv, Mar. 1983, pp. 4.4.2-1–4.4.2-4.
- [6] —, "Generalization of the window method for FIR digital filter design," Technion, Haifa, Israel, EE Publ. 456, Aug. 1983, 47 pp.

## Relationship Between Maximum Likelihood Method and Autoregressive Modeling in Multidimensional Power Spectrum Estimation

FARID U. DOWLA AND JAE S. LIM

**Abstract**—Existence of an exact relationship between the maximum likelihood method (MLM) and autoregressive (AR) signal modeling in multidimensional (m-D) power spectral estimation is shown. For one-dimensional (1-D), uniformly sampled autocorrelation functions (ACF), Burg has shown a relationship between the maximum entropy method (MEM) and MLM spectral estimates. In this note we show a similar relationship between the MLM and AR spectral estimates for m-D (or 1-D) signals sampled nonuniformly or uniformly.

## I. INTRODUCTION

In this paper we show that in m-D power spectrum estimation there is an exact relationship between the MLM spectra and the spectra obtained by AR signal modeling. A special case of this general relationship between the MLM and AR spectra is Burg's [1] result on the relationship between MLM and MEM spectra. For a 1-D uniformly shaped ACF, the case considered by Burg, the MEM spectra and the AR spectra are identical.

Let  $x(\mathbf{p})$  denote a zero-mean homogeneous random field on a m-D lattice  $I^m$ , where  $I$  is the set of integers. Imagine the random field  $x(\mathbf{p})$  being sampled by a set of  $(N+1)$  sensors located at the points  $\mathbf{p}_0, \mathbf{p}_1, \dots, \mathbf{p}_N$ , where  $\mathbf{p}_i \in I^m$ , for  $i = 0, 1, \dots, N$ . It is important to note that there is no restriction in the location of the sensors in  $I^m$  and that the choice of the ordering of the sensors is arbitrary. Making an assumption that  $x(\mathbf{p})$  is ergodic, we have estimates of the m-D correlations given by

$$r_x(\mathbf{p}_i - \mathbf{p}_j) = E[x(\mathbf{p}_i) x^*(\mathbf{p}_j)] = \langle x(\mathbf{p}_i) x^*(\mathbf{p}_j) \rangle \quad (1)$$

for  $0 \leq i, j \leq N$  and where  $E$  denotes the expectation operation, and  $\langle \cdot \rangle$  indicates a time averaging operation. At most  $(N^2 + N + 2)/2$  distinct correlations can be estimated for an array with  $N+1$  sensors. Given the knowledge of these correlations, the problem is to find an estimate of  $P_x(\boldsymbol{\omega})$ , the m-D power spectrum of  $x(\mathbf{p})$  for  $-\pi \leq \boldsymbol{\omega} \leq \pi$ .

It will be shown that the spectral estimates obtained by MLM and AR signal modeling are related by the following identities:

$$\text{MLM}(\boldsymbol{\omega}; \mathbf{p}_N) = \frac{1}{\sum_{n=0}^N \frac{1}{\text{AR}(\boldsymbol{\omega}; \mathbf{p}_n)}} \quad (2a)$$

Manuscript received April 8, 1983. This work was supported in part by the Advanced Research Projects Agency monitored by ONR under Contract N00014-81-K-0742 NR-049-506 and in part by the National Science Foundation under Grant ECS80-07102.